

Density Functional Theory of Hard Sphere Condensation Under Gravity

Joseph A. Both and Daniel C. Hong

Physics, Lewis Laboratory, Lehigh University, Bethlehem, Pennsylvania 18015

Abstract

The onset of condensation of hard spheres in a gravitational field is studied using density functional theory. In particular, we find that the local density approximation yields results identical to those obtained previously using the kinetic theory [Physica A **271**, 192, (1999)], and a weighted density functional theory gives qualitatively similar results, namely, that the temperature at which condensation begins at the bottom scales linearly with weight, diameter, and number of layers of particles.

1 Introduction

In a recent paper, one of the authors (DCH) [1] proposed that hard spheres in the presence of gravitational field, g , undergo a condensation transition, and identified the transition temperature, T_c , as a function of external parameters, i.e.:

$$T_c = mgD\mu/\mu_0 \quad (1)$$

where m and D are the mass and diameter of the hard spheres, μ is the dimensionless layer thickness at $T = 0$, and μ_0 is a constant that reflects the particular manner in which a system packs upon condensing. It was noted that there exists a critical temperature T_c below which the total number of particles is not conserved. This is the temperature at which the density at the bottom layer becomes the close-packed density. Now, since the hard spheres cannot be compressed indefinitely, if the temperature is lowered below T_c , then the first layer should remain at the close-packed state, while the particles at the second layer try to compact themselves and thus crystallize. The crystallization then proceeds upward from the bottom layer as the temperature is lowered. This picture was later confirmed by Molecular

Dynamics simulations [2] for mono-disperse hard spheres and was extended to the segregation of binary mixtures of hard spheres of different mass and diameters [3].

In the original work [1], the Enskog kinetic equation was used to obtain the density profile of hard spheres under gravity. However, in an attempt to solve a highly nonlinear integro-differential kinetic equation, it was assumed that the equilibrium velocity distribution function, $f(\mathbf{r}, \mathbf{v})$, factorizes into a product of space and velocity dependent parts, i.e. $f(\mathbf{r}, \mathbf{v}) = G(\mathbf{r})\phi(\mathbf{v})$ and further that the functional form of $\phi(\mathbf{v})$ is Gaussian, which should be valid for elastic hard spheres. The factorization assumption is an equilibrium ansatz, which states that the configurational statistics are separated out from the kinetics when the system is at equilibrium, so that all the equilibrium quantities can be obtained from the configurational integral of the partition function. The equilibrium state is then the configuration that minimizes the free energy. Therefore, we find it necessary to obtain the results of Ref. [1] by the variational method. Indeed, we will show in this paper that essentially identical results follow from an application of density functional theory (DFT) [5] for liquids to the problem. We will first employ the simplest form of the density functional theory known as the local density approximation (LDA), which assumes that the range of inter-particle interaction is much smaller than the typical length scale on which $\rho(\mathbf{r})$ varies [6]. We will show that the LDA and the Enskog theories are in fact identical, so that in both methods, the condensation temperature is defined as the temperature at which the sum rule breaks down. Next, we will analyze the problem with a simple weighted density approximation (WDA) [6-9], which takes into account the local variation of the density function. In this approximation, the condensation temperature is defined as the temperature at which the volume density at the bottom layer reaches the maximum allowed value. In this approximation, microscopic information is preserved in the density profile; notably the formation of a crystal shows up in the density profile as oscillations. The peak to peak distance of this oscillation is approximately the particle diameter. We will demonstrate that the results of both analyses present a picture identical to those presented in Ref. [1]; in particular we will show how the value μ_0 that appears in Eq. (1) depends on the approximation.

2 Local Density Approximation

The essence of the LDA is to assume that the system may be divided into small pieces of nearly constant density and then to treat each piece as though it were part of a homogeneous system [6]. Under these assumptions one may write a free energy functional:

$$F_{LDA}[\rho] = \int d\mathbf{r} \rho(\mathbf{r}) \psi(\rho(\mathbf{r})) + \int d\mathbf{r} \rho(\mathbf{r}) U_{ext}(\mathbf{r}), \quad (2)$$

where $\psi(\rho(\mathbf{r}))$ is the Helmholtz free energy per particle in the absence of an external field and U_{ext} is the potential energy per particle due to an external field such as gravity. Minimization of this functional under the global constraint that the number of particles is given by

$$N = \int_V d\mathbf{r} \rho(\mathbf{r}) \quad (3)$$

should yield the desired density profile. To be more specific, we define variables for hard spheres of mass m confined in a d dimensional volume $V = L^{d-1}H$ with L^{d-1} being the cross sectional area of a $(d-1)$ dimensional plane and H being the height of the container along which the gravitational field is acting. The Helmholtz free energy per particle consists of two terms,

$$\psi(\rho) = \psi_{id}(\rho) + \psi_{exc}(\rho), \quad (4)$$

where ψ_{id} is the ideal gas contribution,

$$\psi_{id}(\rho) = T(\log(\Lambda^3 \rho) - 1). \quad (5)$$

Note that $\psi_{id} = -T \log(z^N)/N$ with the single particle partition function $z = V(2\pi mT)^3/N!$ [10] and that we have redefined the thermal wavelength $\Lambda \equiv (2\pi mT)^{1/2}$. Next, ψ_{exc} is the excess contribution to the free energy is due to the configurational integral coming from the interactions among particles and is in general written as the integral:

$$\psi_{exc} = T \int_0^\rho \left(\frac{P}{\rho' T} - 1 \right) \frac{d\rho'}{\rho'}, \quad (6)$$

The above equation can be derived from the thermodynamic relation, $P = -(\frac{\partial F}{\partial V})_T$ with the chain rule: $(\frac{\partial}{\partial V})_T = \frac{\rho^2}{N}(\frac{\partial}{\partial \rho})_T$. Note that $P/\rho T - 1$ is the

virial sum. Since gravity acts along the vertical direction z , $U_{ext} = mgz$, and the transverse degrees of freedom can be integrated out to yield the free energy functional per unit area:

$$\begin{aligned} \frac{F_{LDA}[\rho]}{A} \equiv \bar{F}[\rho] &= \int_0^\infty dz \rho(z) \psi_{id}(\rho(z)) + \\ &\int_0^\infty dz \rho(z) \psi_{exc}(\rho) + \\ &mg \int_0^\infty dz \rho(z) z, \end{aligned} \quad (7)$$

where $A = L^{d-1}$ is the cross sectional area in the $x - y$ plane. Minimization of the functional under the constraint Eq. (3) yields an equation for the density profile ρ :

$$\frac{\delta \bar{F}[\rho]}{\delta \rho} = T \log(\Lambda^3 \rho(z)) + \psi_{exc}(\rho) + \rho \frac{d\psi_{exc}}{d\rho} + mgz = \lambda \quad (8)$$

where we have introduced a Lagrange multiplier, λ . Defining $\phi \equiv \rho D^3$ and $\zeta \equiv z/D$, λ should be determined by the sum rule:

$$\mu \phi_c = \int_0^{\phi_0} d\phi \zeta(\phi) = \int_0^\infty d\zeta \phi(\zeta), \quad (9)$$

where ϕ_c is the close-packed density, μ is the number of layers of particles in the system at $T = 0$, and ϕ_0 is the density at the bottom layer. Note that the particular shape of the density profile will depend on the functional form of the pressure P or, equivalently, on the functional form of the excess free energy, ψ_{exc} . One may use the Enskog pressure for hard disks or a hard sphere equation of state given by a functional form:

$$P = \rho T [1 + \gamma \rho D^d \chi(\rho)], \quad (10)$$

where $\chi(\rho)$ is the pair correlation function evaluated at contact ($r = D$), and where $\gamma = \frac{\pi}{2}$ when $d = 2$ and $\gamma = \frac{2\pi}{3}$ when $d = 3$. Then

$$\psi_{exc}(\rho) = \int_0^\rho \gamma \rho' D^d \chi(\rho') \frac{d\rho'}{\rho'}. \quad (11)$$

Substituting this form of ψ_{exc} into Eq. (8) and taking the derivative with respect to z generates, in our non-dimensional variables, the differential equation

$$\frac{d\phi}{d\zeta} + \frac{mgD}{T} \phi = -\gamma \phi \left[\phi \frac{d\chi}{d\zeta} + 2\chi \frac{d\phi}{d\zeta} \right], \quad (12)$$

which is precisely the result obtained in Ref. [1]. Thus the equivalence between the LDA and Enskog theory has been shown, and the constant μ_0 that appears in Eq. (1) can also be derived by the density functional theory in the local density approximation.

To conclude this section we cite some results of the LDA/Enskog theory. Note that for the liquid phase, the density profile $\phi(\zeta)$ in Eq. (9) is a monotonically decreasing function of the height ζ with its maximum value at the bottom. Further, the maximum density ϕ_0 is a function of temperature, too, with the upper bound $\phi_0 \leq \phi_c$. So, the right hand side of Eq. (9) can be written as $f(\phi_0)/\beta$, where $\beta = mgD/T$. The particular form of the function $f(\phi_0)$ depends on the approximation. Ref. [1] (Eq. (15c) and (16c)) gives the functional forms of ϕ_0 in 2d using the Ree and Hoover correlation function [11]

$$\begin{aligned}\chi(\phi) &= \frac{(1 - \alpha_1\phi + \alpha_2\phi^2)}{(1 - \alpha\phi)^2}, \\ \alpha &= 0.489351 \pi/2, \\ \alpha_1 &= 0.196703 \pi/2, \\ \alpha_2 &= 0.006519 \pi^2/4.\end{aligned}\tag{13}$$

and in 3d using the Carnahan-Starling equation of state:

$$\frac{P}{\rho T} = \frac{(1 + \eta + \eta^2 - \eta^3)}{(1 - \eta)^3}.\tag{14}$$

where we have defined the volume fraction $\eta = \frac{\pi}{6}D^3\rho = \frac{\pi}{6}\phi$ in 3d and as $\eta = \frac{\pi}{4}D^3\rho = \frac{\pi}{4}\phi$ in 2d. For completeness, we reproduce these. First, the 2d result:

$$\begin{aligned}f(\phi_0)_{RH} &= (1 + c_2)\phi_0 + \frac{1}{2}c_1\phi_0^2 + \frac{c_3\phi_0}{(1 - \alpha\phi_0)} \\ &\quad - \frac{c_4}{\alpha} \left(\frac{1}{(1 - \alpha\phi_0)} - 1 \right) + \frac{c_4\phi_0}{(1 - \alpha\phi_0)^2}\end{aligned}\tag{15}$$

with $c_1 = \pi\alpha_2/\alpha^2 \approx 0.0855$, $c_2 = -(\pi/2)(\alpha_1/\alpha^2 - 2\alpha_2/\alpha^3) \approx -0.710$, $c_3 = -c_2$, and $c_4 = (\pi/2)(1/\alpha - \alpha_1/\alpha^2 + \alpha_2/\alpha^3) \approx 1.278$. Next, the 3d result:

$$f(\phi_0)_{CS} = \phi_0 - \frac{2\phi_0}{(1 - \alpha\phi_0)} + \frac{2\phi_0}{(1 - \alpha\phi_0)^3},\tag{16}$$

where in this expression $\alpha = \pi/6$. Note that in both 2 and 3 dimensions, $f(\phi_0)$ is a monotonically increasing function of ϕ_0 . Hence, it has a maximum at $\phi_0 = \phi_c$, the value of the close-packed density. Since β or equivalently T and the layer thickness μ are arbitrary control parameters, the sum rule, Eq. (9), breaks down when $T \leq T_c$, where

$$\mu\phi_c = f_{max}T_c/mgD \equiv \mu_0T_c/mgD \quad (17)$$

While the scaling of the critical temperature displayed in Eq. (1) is independent of the particular equation of state used in the calculation, the maximum value of $f(\phi_0)$, μ_0 , depends on the functional form of the density profile, or equivalently, the pressure. Using the two approximations above, and taking the maximum densities as $\eta_c = \frac{\pi}{6}\sqrt{2} \approx 0.74$ in 3d, and $\eta_c = \pi/(2\sqrt{3}) \approx 0.91$ in 2d, we find

$$\begin{aligned} \mu_{0RH} &= 111.31 \quad (2d) \\ \mu_{0CS} &= 152.34 \quad (3d). \end{aligned} \quad (18)$$

At the level of Enskog approximation, μ_0 is quite sensitive to the density at the bottom, ϕ_0 . At this point, we find it appropriate to mention the point made by Levin [16] that reliable information about the fluid-solid coexistence cannot be obtained by the LDA, because of its inability to include the density variations in a highly structured phase (solid). When the Enskog approximation breaks down, one has to either abandon the approximation and search for a better one, or modify the approximation by removing the unphysical results. In the original paper [1], the latter approach was taken, namely based on physical grounds, the crystal regime was replaced by a constant average density, a Fermi rectangle, and the fluid regime was then fit to the Enskog profile, which is linked to the Fermi rectangle at the liquid-solid interface. While the proportionality constant μ_0 in Eq. (1) obtained this way seems to overestimate, and thus while the Enskog equation fails to locate the precise point of the liquid-solid transition, the prediction of its existence and the scaling relation between the critical temperature T_c and external parameters (Eq. (1)) seem to remain true. More elaborate approximations that do take into account the local variations in the structured phase yield substantially lower values for μ_0 (see Fig. 2), which are somewhat close to the values obtained by a Mean Field theory [2]. In order to show the dependence of μ_0 on approximation, we also compute in it 3d by the Percus-Yevick compressibility

form of the equation of state:

$$\frac{P}{\rho T} = \frac{1 + \eta + \eta^2}{(1 - \eta)^3} \quad (19)$$

which yields equally high values for μ_0 ,

$$\begin{aligned} f(\phi_0)_{PYC} &= \frac{\phi_0}{(1 - \alpha\phi_0)} - 3\frac{\phi_0}{(1 - \alpha\phi_0)^2} + \\ &\quad 3\frac{\phi_0}{(1 - \alpha\phi_0)^3}, \\ \mu_{0PYC} &= 185.19. \end{aligned} \quad (20)$$

The slightly different form, namely the virial form

$$\frac{P}{\rho T} = \frac{1 + 2\eta + 3\eta^2}{(1 - \eta)^2}. \quad (21)$$

yields

$$\begin{aligned} f(\phi_0)_{PYV} &= 3\phi_0 - 8\frac{\phi_0}{(1 - \alpha\phi_0)} + 6\frac{\phi_0}{(1 - \alpha\phi_0)^2} \\ \mu_{0PYV} &= 86.63. \end{aligned} \quad (22)$$

We further point out that the breakdown of the sum rule is due to the fact that the pressure has a singularity at $\eta = 1$, and thus it has a *finite* value at the close-packed density η_c , which is necessarily less than one [10]. If one uses the lattice gas pressure [4],

$$P = -T \log(1 - \rho), \quad (23)$$

which has a singularity at $\rho = 1$, then the condensation temperature is zero, and the density profile is given by the Fermi function [5]:

$$\rho(z) = 1/(1 + \exp(mg(z - \mu)/T)) \quad (24)$$

3 Weighted Density Approximation

The essence of the WDA, as introduced by Tarazona [6,7] and Curtin and Ashcroft [8] is to recast Eq. (2), the general form of the free energy functional,

as

$$F_{WDA}[\rho] = \int d\mathbf{r}\rho(\mathbf{r})\psi_{id}(\rho(\mathbf{r})) + \int d\mathbf{r}\rho(\mathbf{r})\psi_{exc}[\rho_w(\mathbf{r})] + \int d\mathbf{r}\rho(\mathbf{r})U_{ext}(\mathbf{r}), \quad (25)$$

where $\psi_{exc}[\rho_w(\mathbf{r})]$ is now a functional of $\rho(\mathbf{r})$, depending on $\rho(\mathbf{r})$ through the weighted average of the density given by

$$\rho_w(\mathbf{r}) = \int d^3\mathbf{r}'w(|\mathbf{r} - \mathbf{r}'|)\rho(\mathbf{r}'), \quad (26)$$

where $w(|\mathbf{r} - \mathbf{r}'|)$ is an appropriately chosen weighting function. Following Tarazona [6], we choose

$$\rho_w(\mathbf{r}) = \frac{3}{4\pi D^3} \int d^3\mathbf{r}'\Theta(D - |\mathbf{r} - \mathbf{r}'|)\rho(\mathbf{r}'), \quad (27)$$

where Θ is the unit step function, i.e., we replace the local density $\rho(\mathbf{r})$ with its average over a sphere of radius equal to the particle diameter D . Because we assume planar symmetry, i.e., independence in the x and y directions, we may integrate out the transverse degrees of freedom and write explicitly the integral above as a one dimensional integral for $z \geq D$:

$$\rho_w(z) = \frac{3}{4D^3} \int_0^\infty dz'\rho(z')(D^2 - (z - z')^2)\Theta(D - |z - z'|). \quad (28)$$

One needs to be careful near the bottom layer $z = 0$, namely, for $0 < z < D$. In this case, the weighting cannot be done over a sphere a radius D , because of the infinite potential at $z = 0$. We propose to carry out the weighting over that *part* of the sphere of radius D and centered at z above the $z = 0$ plane. Thus, the normalization factor, C , that is, the volume over which the integration is performed, is no longer $C = \int_{-D}^D (\pi(D^2 - z'^2))dz' = 4\pi D^3/3$, but instead is $C = \int_{-z}^D (\pi(D^2 - z'^2))dz' = \pi[\frac{2}{3}D^3 + D^2z - \frac{1}{3}z^3]$. Hence, for $z < D$,

$$\rho_w(z) = \frac{1}{[\frac{2}{3}D^3 + D^2z - \frac{1}{3}z^3]} \int_0^\infty dz'\rho(z')(D^2 - (z - z')^2) \times \Theta(D - |z - z'|). \quad (29)$$

As before, we need to extremize the free energy functional under the global constraint on particle number, so we again use the method of Lagrange

multipliers and functional differentiation. Performing the minimization of the free energy functional (Eq. (7) with ρ in the excess term replaced by (28)), we find the following equation must hold:

$$T \ln(\Lambda^3 \rho) + \psi_{exc}(\rho_w(z)) + \int_0^\infty dz' \rho(z') \frac{\delta \psi_{exc}(\rho_w(z'))}{\delta \rho(z)} + mgz + \lambda = 0. \quad (30)$$

We write explicitly the integral term in the equation above:

$$\int_0^\infty dz' \rho(z') \frac{\delta \psi_{exc}(\rho_w(z'))}{\delta \rho(z)} = \int_0^\infty dz' \rho(z') A(z') \times B(z, z') \Gamma(z'), \quad (31)$$

$$A(z') = \frac{d\psi_{exc}(\rho_w(z'))}{d\rho_w(z')}, \quad (32)$$

$$B(z, z') = (D^2 - (z - z')^2) \Theta(D - |z - z'|), \quad (33)$$

$$\Gamma(z') = \frac{3}{4D^3} \quad (34)$$

if $z' \geq D$ and

$$\Gamma(z') = \frac{1}{[\frac{2}{3}D^3 + D^2z' - \frac{1}{3}z'^3]} \quad (35)$$

if $0 < z' < D$.

The integral equation for $\rho(z)$, Eq. (30), is highly nonlinear and complex. Thus, it requires numerical solution. We choose to solve Eq. (30) using the Carnahan-Starling equation of state, Eq. (14), so that

$$A(z') = -\frac{2}{\rho_w(z') \left(1 - \frac{\pi}{6} D^3 \rho_w(z')\right)} + \frac{2}{\rho_w(z') \left(1 - \frac{\pi}{6} D^3 \rho_w(z')\right)^3}. \quad (36)$$

For a given choice of λ we iterate Eq. (30) until the iteration converges to a unique profile. The integral of the profile (Eq. (9)) determines μ , effectively the depth of the unexcited sample, so for fixed m , g , D , and T , we tune λ to control the number of particles.

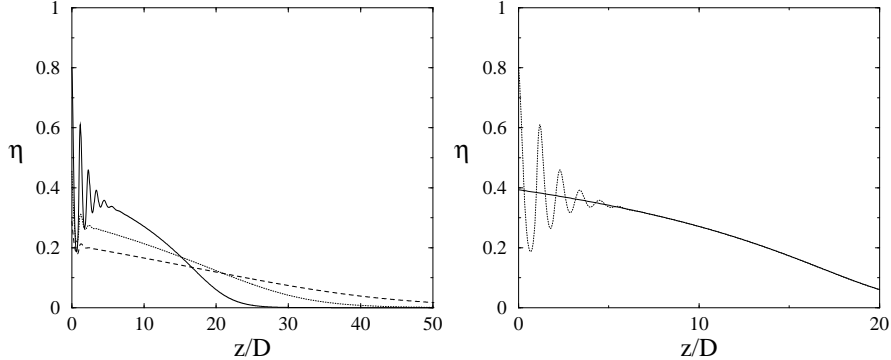


Figure 1: (a) The volume density η as a function of the dimensionless height z/D at different temperatures as calculated from numerical solution of Eq. (30) for given set of m , g , D , and μ . The tail extends as the temperature increases. At high temperature T , the density profile is a monotonically decreasing function of z/D , but as the T approaches the critical temperature T_c , oscillations develop near the bottom, indicating layer formation. (b) The dotted line is a magnified view of the topmost curve in Fig. 1a, while the solid line is the prediction made by the LDA/Enskog theory for the same system.

We find that at high temperatures, the profiles obtained using the WDA match very well the profiles obtained for the same set of parameters using the LDA/Enskog approach. But as we lower the temperature of the system, particles at the bottom begin to compact themselves, and the crystallization sets in. One of the notable features of this weighted density functional approach is that formation of the crystal can be captured in the density profile, in particular oscillations in the density profile appear near $z = 0$. Fig. 1a shows the development of these density peaks for a representative system at three different temperatures above T_c . The peak to peak distance of this oscillation is slightly greater than the diameter of the hard sphere. Fig. 1b is a closer view of the density profile for the coolest of these systems (dotted line). This figure also plots the LDA/Enskog result for the same system (solid line); it agrees well with the WDA profile for large z/D , but cannot reflect the rapid oscillations in density which occur near the bottom of the sample.

With sufficiently low temperature, the bottom-most peaks in the profile

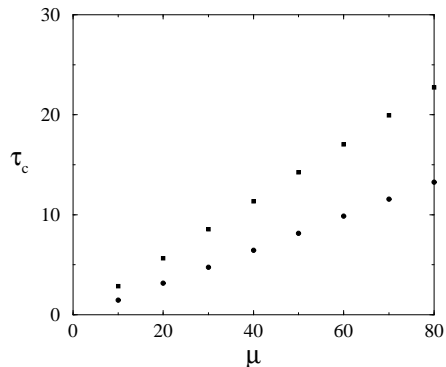


Figure 2: The dimensionless condensation temperature, $\tau_c \equiv T_c/mgD$, is plotted against the dimensionless layer thickness μ . The slope is $1/\mu_0$. Squares are the result for $d = 2$, circles for $d = 3$.

approach (and even exceed) the physical limit of $\eta = 1$. Note that the maximum η for close-packing in 3d is 0.74. However, in our numeric solution, we have chosen the lattice spacing, $\Delta z = D/256$, with D the particle diameter. This choice is to guarantee precision in the solution of the integral equation Eq. (30). Hence, even though the physically relevant limit for the volume fraction η in 3d is 0.74, in our numerical solutions, η must approach one at the close-packed density. With this modification, we define the temperature at which η first reaches this physical limit at $z = 0$ as the critical temperature, T_c . In Fig. 2, for a given set of m, g, D , we have plotted the dimensionless critical temperature $\tau_c \equiv T_c/mgD$ as a function of the initial layer thickness, μ . The numerically determined value from the slope for the constant μ_0 is $\mu_0 = 6.10$ in 3d. We have performed an analogous WDA calculation in 2d using the Ree and Hoover correlation function $\chi(\phi)$, Eq. (13). The data from this calculation also appear in Fig. 2. They yield $\mu_0 = 3.52$ in 2d. Both the 2d and 3d WDA results are smaller than those obtained by the LDA/Enskog approach, and we discuss this next.

As we have discussed, in the LDA/Enskog approach, the value of μ_0 depends on ϕ_0 , the density at the bottom, and is identical to the function $f(\phi_0)$. In all the approximations we have used in this work, $f(\phi_0)$ (see Eqs. (14, 15, 20, 22)) is a function very sensitive to ϕ_0 for ϕ_0 near close-packed values, i.e. for $\phi_0 \geq 1$. Fig. 3a illustrates this sensitive dependence. Molecular dynamics simulations in two dimensions [12] have shown that ϕ_0 at $T < T_c$ varies

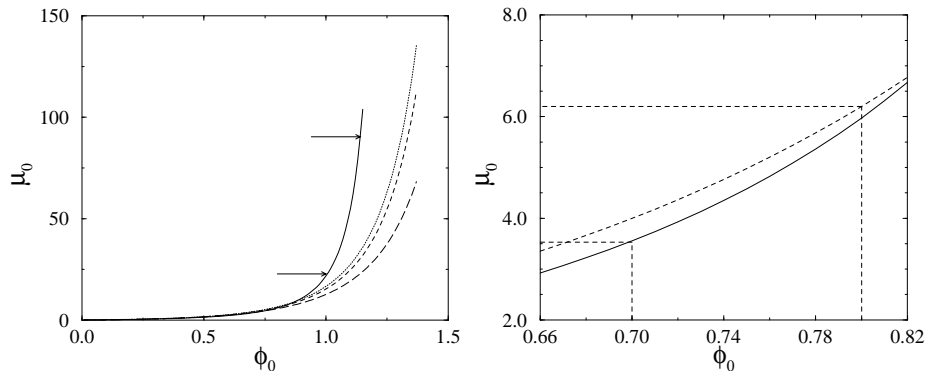


Figure 3: (a) The value $\mu_0 \equiv f(\phi_0)$ as a function of density at the bottom of the sample, ϕ_0 , as calculated in the LDA/Enskog theory. The solid curve is for 2d using the Rees and Hoover value of $\chi(\phi)$, Eq. (15). The remaining curves are for 3d: dotted, Percus-Yevick compressibility form, Eq. (20); dashed, Carnahan-Starling, Eq. (16); long dashed, Percus-Yevick virial form, Eq. (22). The arrows on the 2d curve indicate the range of μ_0 calculated with the LDA/Enskog theory from molecular dynamics simulation values of ϕ_0 . (b) An expanded region of Fig. 3a, showing only the 2d Rees and Hoover curve (solid) and the 3d Carnahan-Starling curve (dashed). See the text for further discussion.

widely. For one set of simulations using 10^3 hard disks with $\mu = 20$, defects in packing lead to ϕ_0 occupying the range $1.00 < \phi_0 < 1.14$, with higher densities occurring at lower temperatures. (Note that for square packing in 2d, $\phi_0 = 1$, while for triangular packing, $\phi_0 = 2/\sqrt{3} \approx 1.155$.) In LDA/Enskog theory, this range of ϕ_0 leads to $21.76 < \mu_0 < 90.33$ (the arrows in Fig. 3a indicate this range), the large range due to the sensitivity of $f(\phi_0)$, while the WDA theory presented here gives a smaller value, $\mu_0 = 3.52$ for the 2d calculation using the same equation of state. Though the discrepancy between the WDA and LDA/Enskog results seems large, the source of the discrepancy is easy to identify. To do so, we first remark that any density profile derived through the WDA for a given system (m , g , D , μ , and T) at temperature below T_c (WDA) differs from the LDA/Enskog profile for the same system appreciably only near the bottom of the sample, where the WDA profile exhibits oscillations and the LDA/Enskog profile is a monotonically decreasing function bounded between the peaks and troughs of the WDA

profile (see Fig. 1b). At the temperature when the bottom-most density peak in the LDA profile reaches its maximum value $\phi_{max} = \frac{4}{\pi}\eta_{max} = \frac{4}{\pi}$, i.e. at T_c (WDA), the LDA/Enskog profile for the same system will have a much smaller maximum. In our work in 2d, at T_c (WDA), the LDA/Enskog profile has $\phi_0 = \frac{4}{\pi}\eta_0 = \frac{4}{\pi} 0.55 \approx 0.70$, below the square packing value, while in 3d, at T_c (WDA), the LDA/Enskog profile has $\phi_0 = \frac{6}{\pi}\eta_0 = \frac{6}{\pi} 0.42 \approx 0.80$, below the simple cubic packing value. If we use these values to compute μ_0 in the LDA/Enskog approach as in Fig. 3b, we get $\mu_0 = 3.56$ in 2d and $\mu_0 = 6.20$, consistent with our determination of μ_0 from the slopes of the lines in Fig. 2. We see then that T_c (WDA) is in general higher than T_c (LDA/Enskog) for the same systems, and this is reflected in the lower value of μ_0 in the former approach.

Finally, we turn our attention to the question of whether the condensation phenomenon we are considering is a phase transition in the thermodynamic sense, i.e., whether condensation corresponds to a discontinuity in the first or higher derivatives of the free energy with respect to temperature. We address this question by focusing on the gravitational potential energy contribution to the free energy, $U_g = mg \int_0^\infty z\rho(z)dz$, which is proportional the center of mass $\langle z \rangle = \int_0^\infty z\rho(z)dz / \int_0^\infty \rho(z)dz$. First we show that in the LDA/Enskog theory, which is extended to temperatures below T_c by the assumption that the density in the frozen layers is given by $\phi = \phi_c$ and that the density above the frozen layers is given by a vertically shifted LDA/Enskog profile [1], a kink in the center of mass develops at $T = T_c$, suggesting a first order transition.

To do this we recall that the density profile $\phi(\zeta)$ is given by the functional form:

$$\beta\zeta = f(\phi) - f(\phi_0) \quad (37)$$

where ϕ_0 is the density at $\zeta = 0$, and $\beta = mgD/T$. Above T_c ,

$$\begin{aligned} \langle \zeta(T) \rangle &= \frac{\int_0^\infty \zeta\phi(\zeta)d\zeta}{\int_0^\infty d\zeta\phi(\zeta)} \\ &\equiv \frac{1}{\beta} I_1 / I_2 \end{aligned} \quad (38)$$

where

$$\begin{aligned} I_1 &= \int_{\phi_0(T)}^0 [f(\phi) - f(\phi_0)]\phi \frac{df}{d\phi} d\phi \\ I_2 &= \int_{\phi_0(T)}^0 \phi \frac{df}{d\phi} d\phi \end{aligned}$$

Now, we note that for T near T_c :

$$\phi_0(T) \approx \phi_c - \alpha(T - T_c) \quad (39)$$

where $\alpha > 0$. Then for any integrand $G(\phi)$ we can make the following approximation:

$$\int_{\phi_0(T)}^0 G(\phi) d\phi \approx \int_{\phi_c}^0 G(\phi) d\phi - \alpha(T - T_c)G(\phi_c). \quad (40)$$

Applying this to the above expression to the integral I_1 and I_2 , we find that $\langle \zeta(T) \rangle$ is linear in T with a quadratic correction.

Below T_c , the density profile develops a kink at $\zeta = L$. For $\zeta < L$, $\phi(\zeta) = \phi_c$ the close-packed density, and for $\zeta > L$, the profile is given by the LDA/Enskog profile Eq. (37), and the thickness of the frozen layer is given by [1]

$$L = \mu(1 - T/T_c). \quad (41)$$

We now compute the center of mass $\langle \zeta(T) \rangle$:

$$\begin{aligned} \langle \zeta(T) \rangle &= \frac{\int_0^\infty \zeta \phi(\zeta) d\zeta}{\int_0^\infty \phi(\zeta) d\zeta} \\ &\equiv \frac{\int_0^L \zeta \phi_c d\zeta + \int_L^\infty \zeta \phi(\zeta - L) d\zeta}{\mu \phi_c} \\ &\equiv \frac{\phi_c L^2/2 + I}{\mu \phi_c} \end{aligned} \quad (42)$$

where

$$\begin{aligned} I &= \int_0^\infty \zeta \phi(\zeta) d\zeta + L \int_0^\infty \phi(\zeta) d\zeta \equiv I_1 + LI_2 \\ I_2 &= \phi_c(\mu - L). \end{aligned} \quad (43)$$

Hence,

$$I = \phi_c \mu^2 \frac{T}{T_c} \left(1 - \frac{T}{T_c}\right) + J$$

where

$$J = \int_0^\infty \zeta \phi(\zeta) d\zeta = \int_{\phi_c}^0 \zeta(\phi) \phi \frac{d\zeta(\phi)}{d\phi} d\phi \equiv \Lambda/\beta^2 \propto T^2$$

and where

$$\Lambda = \int_0^{\phi_c} [f(\phi_c) - f(\phi)] \phi \frac{df(\phi)}{d\phi} d\phi.$$

It therefore follows that

$$\langle \zeta(T) \rangle = \frac{\mu}{2} + \lambda_1 T^2 \quad (44)$$

where

$$\lambda_1 = \left[\frac{1}{\mu} \left(\frac{1}{mgD} \right)^2 \left(\frac{\Lambda}{\phi_c} - \frac{\mu_0^2}{2} \right) \right].$$

The center of mass scales with temperature quadratically below T_c but linearly just above T_c ; thus, there is a kink in the center of mass and in the gravitational potential energy contribution to the free energy, giving rise to a first order transition.

The scaling of $\langle \zeta \rangle$ with T^2 below T_c survives a modification of how we represent the frozen region. Suppose, the density in the frozen region is not represented by a uniform ϕ_c but is instead given by

$$\phi(\zeta) = \sum_i p_i \delta(\zeta - \zeta_i) \quad (45)$$

where ζ_i is the position of the center of hard spheres and p_i is its peak density in the i -th row forming a crystal. This is a crude way to approximate the oscillations in the density profile due to the crystallization. Then, I_1 in Eq. (43) is replaced by:

$$I_1 = \int_0^L \zeta \phi(\zeta) d\zeta = \sum_i \zeta_i p_i \quad (46)$$

If $p_i = \phi_c$ for all i , then,

$$\begin{aligned} I_1 &= \phi_c \sum_i \zeta_i = \phi_c [1/2 + 3/2 + 5/2 + \dots + (2L - 1)/2] \\ &= \phi_c L^2 / 2 \end{aligned} \quad (47)$$

which is the same result as that obtained by assuming the density profile is approximated by a Fermi rectangle.

The WDA approach to the problem also yields results suggestive of the existence of a first order phase transition. It may be an artifact of the method that in the WDA solutions, as T is lowered below T_c as we have defined it, large density peaks whose maxima exceed the physical limit $\eta = 1$ appear. Thus the WDA does not capture the exact distribution of material in the system. However, it is nonetheless suggestive to examine the dependence of the center of mass $\langle \zeta(T) \rangle$ on T . Fig. 4 shows results for a representative

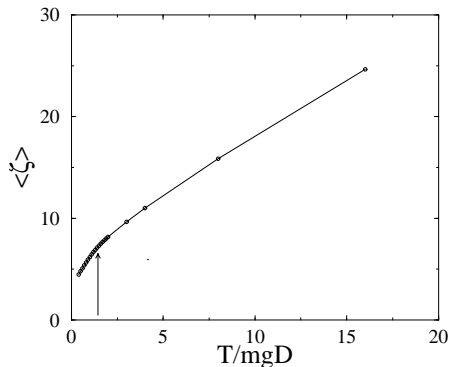


Figure 4: WDA calculation of center of mass $\langle \zeta \rangle$ vs. T/mgD for a system with $\mu = 10$. The arrow indicates T_c and points to what may be a kink in the function.

system in 3d with $\mu = 10$ and whose critical temperature was found to be on the range $1.4 mgD < T_c < 1.5 mgD$. An elbow, possibly a kink, is apparent in the vicinity of T_c , marking the onset of near linear behavior for $T > T_c$. We do not assert that this is evidence of a phase transition; we display this data merely to suggest that the existence of such a phase transition in the WDA approach is not inconsistent with our data. A different form for the weight function in Eq. (26) might yield a better result regarding the nature of the phase transition.

4 Conclusions

We have shown that the conclusion of the original paper [1], namely, that the scaling of the critical temperature at which hard spheres under gravity begin to form a solid is linear with their weight, their diameter, and the depth of the sample, necessarily follows from the simplest density functional theory for the problem (the LDA) and survives a richer density functional treatment using a WDA. Prudence requires us to note that our WDA for this problem did not include any sophisticated attempt to represent the crystal-fluid interface, something other researchers [13-15] working on similar problems have done. Doing so should likely give a more accurate quantitative picture than that presented here.

Acknowledgment

The authors wish to thank Y. Levin for helpful discussion over the course of this work.

References

- [1] D. C. Hong, *Physica A* **271**, 192 (1999).
- [2] P. V. Quinn and D. C. Hong, cond-mat/0005196.
- [3] D. C. Hong, P. V. Quinn and S. Luding, cond-mat/0010459.
- [4] D. C. Hong and K. McGouldrick, *Physica A* **255**, 415 (1998).
- [5] H. Hayakawa and D. C. Hong, *Phys. Rev. Lett.* **78**, 2764 (1997).
- [6] P. Tarazona, *Mol. Phys* **52**, 81 (1984).
- [7] P. Tarazona, *Phys. Rev. A* **31**, 2672 (1985).
- [8] W. A. Curtin, N. W. Ashcroft, *Phys. Rev. A* **32**, 2909, (1985).
- [9] A. Diehl, M. N. Tamashiro, M. C. Barbosa , and Y. Levin, *Physica A* **274**, 433 (1999).
- [10] J. P. Hansen and I. R. McDonald, *Theory of Simple Liquids*, Academic Press, New York, 1976.
- [11] F. R. Ree, W. G. Hoover, *J. Chem. Phys.* **40**, 939, (1964).
- [12] P. V. Quinn, private communication.
- [13] R. Ohnesorge, H. Lowen, and H. Wagner, *Phys. Rev. A* **43**, 2870 (1991).
- [14] R. Ohnesorge, H. Lowen, and H. Wagner, *Phys. Rev. E* **50**, 4801 (1994).
- [15] T. Biben, R. Ohnesorge, and H. Lowen, *Europhys. Lett.* **28**, 665, (1994).
- [16] Y. Levin, *Physica A* **287**, 100, (2000).